

Toward Real-World Pathological Voice Detection

Heng-Cheng Kuo, Yu-Peng Hsieh, Huan-Hsin Tseng, Chi-Tei Wang, Shih-Hau Fang, and Yu Tsao, *Senior Member, IEEE*

Abstract—Voice disorders significantly undermine people’s ability to speak in their daily lives. Without early diagnoses and treatments, these disorders may drastically deteriorate. Thus, automatic detection systems at home are desired for people inaccessible to disease assessments. However, more accurate systems usually require more cumbersome machine learning models, whereas the memory and computational resources of the systems at home are limited. Moreover, the performance of the systems may be weakened due to domain mismatch between clinic and real-world data. Therefore, we aimed to develop a compressed and domain-robust pathological voice detection system. Domain adversarial training was utilized to address domain mismatch by extracting domain-invariant features. In addition, factorized convolutional neural networks were exploited to compress the feature extractor model. The results showed that only 4% of degradation of unweighted average recall occurred in the target domain compared to the source domain, indicating that the domain mismatch was effectively eliminated. Furthermore, our system reduced both usages of memory and computation by over 73.9%. We concluded that this proposed system successfully resolved domain mismatch and may be applicable to embedded systems at home with limited resources.

I. INTRODUCTION

Early epidemiology study had reported varying estimates on the prevalence of dysphonia, ranging from 0.65% to 15% [1], [2]. Later report had estimate the prevalence among US to be around 3% to 9% [3]. Recently, a regional telephone survey of 1326 random subjects revealed a current voice disorder of 6.6% and a lifetime prevalence of 29.9% in adults aged less or equal to 65 years [4]. Another study based on primary care physicians had demonstrated similar result on life time prevalence of dysphonia (4.3% to 29.1%) and 7.5% of current voice disorders [5]. More recently, two large-scaled claim data-based epidemiological studies had revealed the prevalence rate of voice disorders ranging from 0.26% to 0.98% [6], [7]. All researches indicated that the overall prevalence of voice disorders is quite alarming. For such disease, accurate diagnoses usually require experienced specialists and expensive equipment. Owing to the lack of health insurance or other medical resources, adequate disease assessments are often inaccessible for people in need. Therefore, an automatic detection system helping individuals to detect the existence and/or the type of pathological voice at home is desired.

To tackle this problem, several noninvasive screening methods were proposed and the potential to detect samples of pathological voice had also been demonstrated in [8]–[10]. Furthermore, pathological voices always accompany changes of voice quality, so speech signal processing methods were widely utilized to improve the accuracy of pathological voice detection, such as time-frequency approaches [11], Mel frequency cepstral coefficients (MFCCs) [12], MFCCs with Gaussian mixture models (GMM) [13], MFCCs with hidden

Markov model (HMM) [14], and wavelet coefficients [15]. In recent decades, traditional machine-learning-based algorithms had been also investigated. For example, support vector machine (SVM) [16]–[23], Naive Bayes [24], and k-nearest neighbors (KNN) [25] all achieved outstanding performances. On the other hand, Wu *et al.* [26], [27], Gupta *et al.* [28] and Fang *et al.* [29] verified the reliability of neural network (NN) by various NN-based models. Automatic speech recognition system was exploited to assess voice disorders as well [30]. On the basis of great performance, Hsu *et al.* [31] further dealt with the channel effect due to hardware variation. In addition to above research, the FEMH Challenge was internationally held by the IEEE Big Data conference in Seattle 2018, in which numerous groups built pathological voice detection systems [32]–[37] based on the same evaluation metrics and the same dataset published by Far Eastern Memorial Hospital (FEMH), Taiwan [38].

However, current NN solutions are not optimal in practical applications due to two main challenges. First, model structures of neural networks are usually designed large to achieve state-of-the-art performances. On the other hand, limited memory and computational resources of embedded system allow little room for models to increase parameters. Second, the domain mismatch between training and testing data acquired from real-world scenarios substantially degrades the accuracy.

Owing to that a large model requires huge memory capacity and computational resource, there are typically three common solutions to achieve real-time processing on embedded systems, including quantization technique, knowledge distillation and factorized convolutional neural network (CNN). Quantization is a technique to replace arithmetic of 32-bit floating points with that of integers [39] or powers of two [40], implemented with much lower latency on commonly available hardware. Moreover, representations of even lower bits can be applied due to the limited amount of quantized values, so that it further reduces the usage of memory. Another solution, knowledge distillation, is the process of transferring the knowledge from a large network, especially for an ensemble of models, to a small one [41]. The outputs generated by the cumbersome but well-trained network act as additional targets of distilled network. Thus, it can achieve better performance than only using the true labels as targets. Last but not least, the standard CNN can be considered as a combination of spatial convolution in each channel, also called *intra-channel convolution*, and linear projection across channels simultaneously [42]. Therefore, using the factorized CNN can reduce its memory or computation by rearranging the spatial convolution or dealing with these two parts separately. The Efficient Residual Factorized Network (ERFNet) [43] factorizes the 3×3 convolution into the union of perpendicular

3×1 and 1×3 convolutions, and residual connections are used to improve training efficient while retaining remarkable accuracy. Another factorized network, MobileNet, is aimed for mobile and embedded vision applications [44]. It is based on a streamlined architecture, separable convolution which is composed of a depth-wise convolution (intra-channel convolution) and a 1×1 point-wise convolution (cross-channel projection), to build light weight deep neural networks. In addition, two simple global hyper-parameters are introduced to trade off between latency and accuracy efficiently.

Another issue in real-world scenario is the domain mismatch. Although joining abundant labeled data of different environments is likely to improve the generalizability for models, it is not feasible to prepare rather diverse and out-of-clinic data in biomedical area due to extreme time consumption. Additionally, labeling such data requires strong professional backgrounds which further increase the difficulty. As the unsupervised domain adaptation method is trained on labeled data from the source domain and unlabeled data from the target domain, it intends to learn features minimizing the distance between the probability distributions of the source and the target domain. Therefore, a unsupervised domain adaptation method allows us to directly apply a well-trained model to the target domain to fit our purpose. For deriving domain-invariant features, Tzeng *et al.* [45] introduced Maximum Mean Discrepancy (MMD) to compute the distance between domains and minimize MMD and classification loss together. Another method, domain adversarial training (DAT), augments the original NN architecture with a domain classifier and a gradient reversal layer (GRL) [46]. The domain classifier is trained to discriminate features between source and target domains, but original NN architecture is updated adversarially with negative gradient produced by GRL to fool the domain classifier. This adversarial process encourages domain-invariant features to emerge.

In this paper, we propose a new pathological voice detection system customized for embedded devices and the system adapts to daily noisy environments simultaneously. The proposed model consists of factorized CNN to obtain compact architecture and is augmented with a DAT module during training to equip the ability of being operated in noisy environments. The paper is organized as follows: in Section II, the details of our system are described, including the MobileNet and the DAT. The experimental results and an ablation study are presented in Section III. Finally, discussions are concluded in Section IV.

II. METHODOLOGY

A. Model compression

In order to realize the high penetration rate of self-diagnosis at home, our detection system will confront the limitation of computation and memory resources on embedded devices, so that, in addition to accuracy, computation cost and model size are also prior considerations. Our first treatment reducing the difficulties is to replace standard convolutional layers with separable convolutional layers in the model construction. A separable convolutional layer [44] is defined to factorize the

standard convolutional layer into a depth-wise convolutional layer and a point-wise convolutional layer

As is known, a standard convolution Fig. 1(a) deals with spatial convolution in each channel and linear transformation across channels simultaneously, while a separable convolution splits this operation into two stage. Specifically, in the first stage the depth-wise convolution Fig. 1(b) is applied a single filter to per each input channel, and in the second stage the point-wise convolution (simply a 1×1 convolution) Fig. 1(c) then performs a linear projection on the previous depth-wise convolution outputs. Attributed to separately considering the relation in each channel and the relation between channels, the computation and model size are drastically reduced.

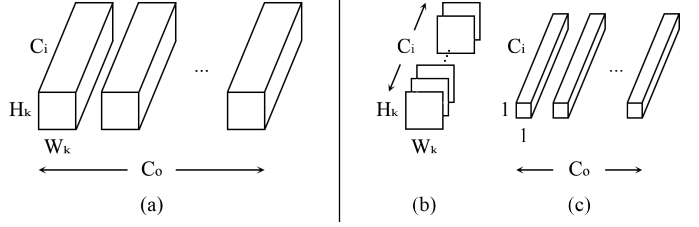


Fig. 1. (a) The standard convolutional filters with factorization into (b) the depth-wise convolutional filters for intra-channel convolution and (c) the point-wise convolutional filters for cross-channel projection.

Consider a general 3D input $\mathbf{I} \in \mathbb{R}^{W_i \times H_i \times C_i}$, an output $\mathbf{O} \in \mathbb{R}^{W_o \times H_o \times C_o}$ and a corresponding convolution kernel $\mathbf{K} \in \mathbb{R}^{W_k \times H_k \times C_i \times C_o}$ in the standard convolutional layer, where W_i , H_i and C_i denote the width, height and number of channels of an input feature respectively; similarly W_o , H_o , C_o , W_k , H_k denote those of an output feature and a convolution kernel. In the following, a filter is defined by a group of kernel parameters decomposed along the dimension of output channels. Therefore, \mathbf{K} is regarded as C_o filters of size $W_k \times H_k \times C_i$.

Because a standard convolutional layer is parameterized by its convolution kernel \mathbf{K} , we can directly derive the amount of parameters in a single layer, Fig. 1(a):

$$W_k \cdot H_k \cdot C_i \cdot C_o \quad (1)$$

On the other hand, due to only intra-channel convolutions, a convolution kernel $\hat{\mathbf{K}}$ of the depth-wise convolutional layer is comprised of C_i filters of size $W_k \times H_k$. Moreover, the number of channels for the output features remains C_i . Therefore, a point-wise convolutional layer combining the information between channels and mapping to desired shape is essential. Since we focus on the convolutions across channels, the width and height of point-wise convolution kernel $\check{\mathbf{K}}$ are set to 1, forming a 1×1 convolutional layer. In total, the amount of parameters of a separable convolutional layer is:

$$W_k \cdot H_k \cdot C_i + 1 \cdot 1 \cdot C_i \cdot C_o \quad (2)$$

By Eq. (1), (2), the reduction ratio of the model size is:

$$\frac{W_k \cdot H_k \cdot C_i + 1 \cdot 1 \cdot C_i \cdot C_o}{W_k \cdot H_k \cdot C_i \cdot C_o} = \frac{1}{C_o} + \frac{1}{W_k \cdot H_k} \quad (3)$$

Next, we discuss the reduction of computation. The computation cost is dominated by multiplications of floating points,

so we analyze the number of multiplications in convolutional layers. Since each element on the output feature is the dot product of the specific filter and part of the input feature, the number of multiplications is the filter size times the output dimension. The point-wise convolutions merely affect the dimension of channels, and hence the output feature of depth-wise convolutional layer sizes $W_o \times H_o \times C_i$ after intra-channel convolutions. The following are computation costs for each type of convolution layer:

$$\begin{aligned} \text{Standard:} & (W_k \cdot H_k \cdot C_i) \cdot (W_o \cdot H_o \cdot C_o) \\ \text{Depth-wise:} & (W_k \cdot H_k) \cdot (W_o \cdot H_o \cdot C_i) \\ \text{Point-wise:} & (1 \cdot 1 \cdot C_i) \cdot (W_o \cdot H_o \cdot C_o) \end{aligned} \quad (4)$$

The computational reduction ratio is then:

$$\begin{aligned} & \frac{(W_k \cdot H_k) \cdot (W_o \cdot H_o \cdot C_i) + (1 \cdot 1 \cdot C_i) \cdot (W_o \cdot H_o \cdot C_o)}{(W_k \cdot H_k \cdot C_i) \cdot (W_o \cdot H_o \cdot C_o)} \\ & = \frac{1}{C_o} + \frac{1}{W_k \cdot H_k} \end{aligned} \quad (5)$$

Eq.(3) and (5) reveals that the model size and the computational cost can both be significantly reduced over 73% in our design. More experimental details can be found in Section III-B.

B. Domain adaptation

Compared to the undisturbed clinics or studios where the pathological voices are recorded, the background noise is inevitable in daily life where our system is aimed at using. Moreover, there are very few annotated data in out-of-clinic scenarios available, since it is hard to perform standard and unified experiments for the general public without the assistance of experienced specialists. Thus, dealing with domain mismatches between training and testing data poses a challenge.

In general, the training data defined as the *source domain* has one probability distribution, while the testing data called the *target domain* has another. They are expected to be similar yet different. In this work, an unsupervised domain adaptation method called the Domain Adversarial Training (DAT) [46] is applied in our detection system to tackle domain mismatch problems.

A pathological voice detection model consists of two parts, a feature extractor and a disease predictor. The feature extractor is designed to extract useful information from the input utterances; subsequently the disease predictor utilizes the extracted features for disease diagnosis. Several domain adaptation techniques typically rely on a feature extractor deriving features invariant across domains, *e.g.*, ignoring the background noise or the difference between recording devices [31], so that a model can generalize on the target domain while preserving a low risk of misclassification on the source domain. The following is how *invariant* is defined in this paper: if the extracted features perplex the domain classifier at all times, those features are then considered *invariant* across domains. On this idea, DAT introduces a domain classifier to assess the domain invariability of the extracted features. It remains to train a domain classifier to derive such features.

The method of DAT to fool the domain classifier is to update the feature extractor in the opposite direction of minimizing the domain classification loss. As such, the training phase can be written as a min-max algorithm:

$$\arg \max_{\theta_d} \min_{\theta_f, \theta_y} \mathbb{E}_{x \sim D_s} [L_y] + \mathbb{E}_{x \sim D_s \times D_t} [-\lambda L_d] \quad (6)$$

$$L_y = -\log P(\mathbf{y} | \mathbf{x}, \theta_f, \theta_y) \quad (7)$$

$$L_d = -\log P(\mathbf{d} | \mathbf{x}, \theta_f, \theta_d) \quad (8)$$

where a data point $\{\text{input utterance, label, domain}\}$ is denoted by $\{\mathbf{x}, \mathbf{y}, \mathbf{d}\}$, and $\theta_f, \theta_y, \theta_d$ denote the parameters of feature extractor, disease predictor and domain classifier respectively. L_y denotes the cross entropy loss of the labels, and L_d is that of the domains; D_s and D_t denote the source domain and the target domain data distribution with $\lambda \geq 0$ as the coefficient regularizing the loss Eq. (6). To improve the performance of main task, detection of pathological voice, the feature extractor and the disease predictor shall jointly minimize L_y . Due to the unsupervised domain adaptation scheme, L_y can only be computed on source domain data. On the other hand, the domain classifier minimizes L_d to enhance the ability of discriminating domains, whereas the feature extractor maximizes L_d to get the opposite gradients. For simplicity, we substitute $-L_d$ for L_d in Eq.(6) and invert minimizing and maximizing operations correspondingly.

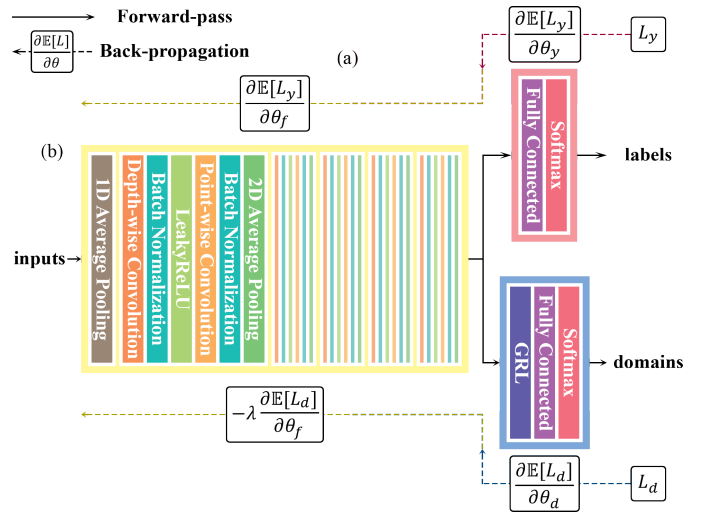


Fig. 2. The proposed architecture includes a feature extractor (yellow) and a disease detector (red) to detect the pathological voices. A domain classifier (blue) is placed after feature extractor for learning domain-invariant features in the unsupervised scheme. (a) As Eq. (11) to Eq. (13), we minimize the label prediction loss L_y and the domain classification loss L_d as usual but when updating feature extractor, the gradient comes from L_d is multiplied by a negative coefficient, $-\lambda$, via GRL during back-propagation. (b) The feature extractor consists of 5 separable convolutional blocks; The disease detector and domain classifier are simply combinations of a fully connected layer and a softmax layer.

For realizing the adversarial min-max Eq.(6), we first formulate the updates of parameters θ_f, θ_y and θ_d via gradient

descent [47] as follows:

$$\theta_f \leftarrow \theta_f - \alpha \left(\frac{\partial \mathbb{E}[L_y]}{\partial \theta_f} - \lambda \frac{\partial \mathbb{E}[L_d]}{\partial \theta_f} \right) \quad (9)$$

$$\theta_y \leftarrow \theta_y - \alpha \frac{\partial \mathbb{E}[L_y]}{\partial \theta_y} \quad (10)$$

$$\theta_d \leftarrow \theta_d - \alpha \lambda \frac{\partial \mathbb{E}[L_d]}{\partial \theta_d} \quad (11)$$

where α denotes the learning rate. Figure 2(a) visualizes the gradient descent process. The updates of Eq.(9) and (11) is observed to differ by a minus sign on partial differential of L_d . The study of DAT introduced a novel gradient reversal layer (GRL) represented by two functions R and \tilde{R} at different stages requiring no parameters such that:

$$\begin{aligned} R(\mathbf{z}) &= \mathbf{z} && \text{(forward propagation)} \\ \tilde{R}(\mathbf{z}) &= -\mathbf{z} \Leftrightarrow \nabla_{\mathbf{z}} \tilde{R} = -\mathbf{I} && \text{(backward propagation)} \end{aligned} \quad (12)$$

where \mathbf{z} and \mathbf{I} denote the input and identity matrix respectively. It should be noted that a general layer with forward function $\mathbf{z} \mapsto f(\mathbf{z})$, the backward propagation naturally has derivative $\mathbf{z} \mapsto \nabla_{\mathbf{z}} f$ from the same f . The GRL deliberately splits the forward and backward function into two to achieve the designated purpose. As such, the GRL acts as an identity function during the forward propagation, but multiplies the gradient by -1 during back propagation. Owing to the GRL, the DAT algorithm can be implemented on any existing machine-learning package with little effort.

Besides its outstanding performance, another reason to use DAT as the domain adaptation method in our system is that it does not increase any memory load or computational cost in the testing phase. During the training phase, the feature extractor collaborates with the domain classifier to jointly learn domain-invariant features. However, in the testing phase, the disease predictor utilizes the well-trained features from both domains to diagnose diseases without the interference of the domain classifier. Thus, the number of parameters remains unchanged regardless of whether the DAT technique is used.

C. Model Architecture

Figure 2(b) shows the proposed pathological voice detection system. The feature extractor consists of separable convolutional layers receiving inputs of size (127, 251) with the first and second dimension denoting the *frame length* and the *frequency basis*, respectively. First 1D average-pooling layer (with kernel size 2 and stride 2) then reduces the input size along the dimension of frequency to be (127, 126), leaving the frame length unchanged. Subsequently, the down-sampled inputs are extended with a dimension of channels to be (127, 126, 1). After the first 1D average-pooling layer, five identically separable convolutional blocks follow, where each of which comprises a depth-wise convolutional layer (kernel size (3, 3, C_i) and stride 1), a point-wise convolutional layer (kernel size (1, 1, C_i , 16) and stride 1) and a 2D average-pooling layer (kernel size 2, stride 2). Here, C_i sets to 1 in the first block and 16 in the rest. Batch normalizations [48] are placed after all convolutional layers (depth-wise and

point-wise), while LeakyReLUs [49] (negative slope = 0.2) are inserted after depth-wise convolutional layers only. The final output of the feature extractor, viewed as a 1D vector of dimension 256, is regarded as the extracted feature carrying domain invariant information to pass on to the next disease predictor and the domain classifier. The disease predictor is a fully connected layer of matrix size (256, k) with a softmax layer concatenated right after to predict the probability between the k distinct diseases, in our case $k = 3$ (normal, Neoplasm, and Phonotrauma).

The domain classifier is similar to the disease predictor only with the last fully-connected layer size replaced by (256, 2) for binary classification and augmented with a GRL ahead. Incidentally, the ADAM [50] optimizer at learning rate 0.001 and the regularization coefficient $\lambda = 0.5$ are used throughout the experiments unless otherwise specified.

III. EXPERIMENTS

A. Dataset and Preprocessing

The voice samples were collected from the Far Eastern Memorial Hospital (FEMH) by a unidirectional microphone and a digital amplifier (CSL model 4150B, kay Pentax). All patients uttered a sustained vowel /:a/ for at least 2 seconds in the samples. The sampling rate was 44.1 kHz with a 16-bit resolution and data were saved in an uncompressed wave format.

523 voice samples were recorded in a voice clinic as the source domain containing 108 normal voices, 112 glottic neoplasms and 303 phonotraumatic diseases (*i.e.*, vocal nodules, polyps and cysts). Another 30 voice samples, 10 of each category, were synthesized with various noises of air conditioners as the target domain data, where the labels were not provided during training phase.

In this study, a 5-fold cross-validation approach was applied to validate the proposed system [51]. Specifically, 523 speech samples were randomly selected and divided into 5 equal partitions and each partition served as the testing fold in turns. Such approach can reduce the bias (resulting from the environment) to evaluate the system. In Section III-B, all scores reported were the averages of 5 folds. The voice samples in the testing fold were inferred under both the source domain in the clinic and the target domain under noises of air conditioners to assess the effect of our system. Here, it should be emphasized that the patients and the magnitudes of noises in target domain were totally distinct between the training and testing phases, SNR (signal-to-noise ratio): 0, 5, 10 dB for training and 3, 6, 9 dB for testing.

Prior to training, the raw waves were first down sampled from 44.1 kHz to 16 kHz and subsequently converted into Log Power Spectrums (LPSs) using Hamming filter, 31.25 ms window size, and half of the window size as the shift of frame. The LPSs were normalized by standard score before fed to the models. During training, random segments of 127 frames (2 seconds) from the normalized LPSs were chosen as inputs every training epoch, to increase the training variety for models. During testing, however, the first 2 seconds of the normalized LPSs were fixed as inputs.

TABLE I
COMPARISON OF SEP CONV-30 WITH ITS ‘‘SUPERVISED’’ VARIANTS FOR DOMAIN ADAPTATION.

Model	Source Domain				Target Domain			
	Normal	Neoplasm	Phonotrauma	UAR	Normal	Neoplasm	Phonotrauma	UAR
StdConv	0.93	0.83	0.81	0.86	0.68	0.79	0.42	0.63
SepConv	0.91	0.79	0.82	0.84	0.58	0.84	0.43	0.62
SepConv-tgt	0.46	0.64	0.83	0.64	0.60	0.72	0.65	0.66
SepConv-ft	0.80	0.73	0.80	0.78	0.71	0.81	0.56	0.69
SepConv-jnt	0.93	0.73	0.70	0.79	0.81	0.80	0.65	0.75
SepConv-30	0.82	0.81	0.74	0.79	0.76	0.83	0.70	0.76

TABLE II
RESOURCE USAGE FOR REPLACING STANDARD CONVOLUTIONS WITH SEPARABLE CONVOLUTIONS.

Model	# Parameters ($\times 10^3$)	# MACs ($\times 10^6$)
StdConv	10.29	15.82
SepConv	2.69	3.64

B. Results

Table I shows the overall performances of various baselines and the proposed method. First, we verify the effectiveness of separable convolutional layers **SepConv**. **SepConv** is similar to the architecture mentioned in Section II-C with the domain classifier removed and only source domain data are used during training. **StdConv**, on the other hand, replaces the separable convolutional layers in **SepConv** with standard ones such that the argument of the input channels, output channels, kernel size, etc. are identical in these two baselines. Table I shows that the degradation is insignificant in **SepConv** with Unweighted Average Recalls (UARs) reduced only by 2% in the source domain and 1% in the target domain when compared to **StdConv**. Without dropping performance in UARs, **SepConv** significantly reduces model size and computational cost, by 73.9% in number of parameters and 77.0% in number of Multiply-Accumulate Operations (MACs) from Table I. Thus, in the following domain adaptation experiments **SepConv** will be the basis for comparison. On the other hand, the two baseline scores also show that the noises of air conditioners tend to make the models misjudging the noisy inputs as neoplasms without domain adaptation.

Our proposed system based on **SepConv** with 30 target domain samples provided in the DAT is denoted by **SepConv-30**. Another three ‘‘supervised’’ variants are constructed for systematic comparison: **SepConv-tgt**, **SepConv-ft** and **SepConv-jnt**, with the architecture fixed as **SepConv** yet the training strategies slightly altered as follows:

- **SepConv-tgt**: the model is trained *only on the 30 target domain samples with labels* provided. In turn, the target domain is an exposed domain to **SepConv-tgt**, yet the source domain becomes unseen.
- **SepConv-ft**: this variation uses a pretrained **SepConv** as an initial state then gets fine-tuned using the 30 target

samples with labels.

- **SepConv-jnt**: train **SepConv** from scratch with labeled data jointly from both domains.

It is observed that **SepConv-30** outperforms all baselines in target data UAR and almost match that of source data, particularly the other systems **SepConv-tgt**, **SepConv-ft**, **SepConv-jnt** with extra labels of target data provided. Comparing to **SepConv**, the UAR increases 14% in target data, only with slight degradation in source domain maintaining 79%.

In **SepConv-tgt**, there is no doubt that the target data UAR is better than that of source data due to the exposed target domain. However, the UAR of **SepConv-tgt** in the exposed (target) domain is not comparable with that of **SepConv** in the exposed (source) domain; the reduction is up to 18%. Moreover, this UAR in the exposed (target) domain is even worse than that of other compared systems in the unseen (target) domain. The poor performance reflects the impact of small size in dataset.

The fine-tuning of **SepConv-ft** successfully improves the UAR in the target domain by 7% but the degradation in source domain is also obvious. The average UARs of **SepConv-ft** is almost equal to that of **SepConv**, which means we simply got trade off between the two domains. The model generalizability is not fully achieved by fine-tuning on limited data in the target domain.

Intuitively, **SepConv-jnt** should achieve the best performance with sufficient data in both domains. However, due to extreme small target data under the proposed scenario, severe imbalance of the two domains confines the improvement of generalizability. Finally, the total scores of **SepConv-jnt** still worse than our proposed **SepConv-30**.

C. Ablation: the impact of the domain classifier via λ

We conduct an ablation study to learn how the regularization coefficient λ in Eq. (9) and (11) affects the domain adaptation performance. Owing to the unstable training procedure of adversarial min-max method, the statistics of 200 models with random initialized weights were considered for each setup in the ablation experiment. Figure 3 only shows the results of a specific fold, but the other folds are similar.

The coefficient λ were tuned from 0.01 to 5 to understand the effect. The results in Figure 3 indicated that when $\lambda \geq 5$,

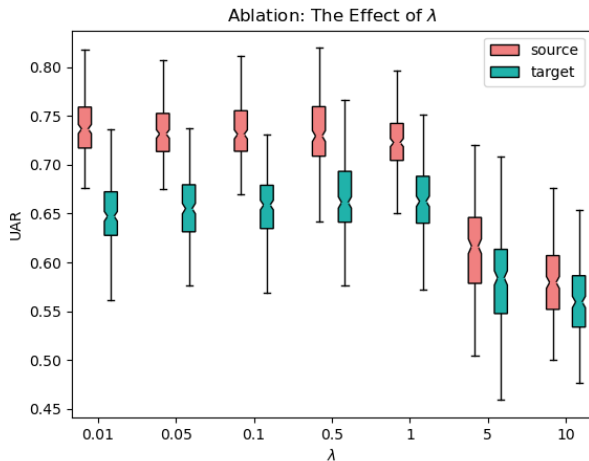


Fig. 3. Box plots of different λ .

the UAR performances in both domain broke down promptly. It was due to the gradient of L_d over amplified by large λ such that the overall update were guided away from the direction of minimizing L_y to affect the diagnosis prediction. On the other hand, the observed fact that when $\lambda \rightarrow 0$ the less domain-invariant the features are meets our intuition. The coefficient is somewhere between $[0, 5]$ to best construct domain invariant features. In this study, $\lambda \leq 0.5$ was observed to yield converging UARs in source data, so that $\lambda = 0.5$ was eventually chosen to balance the accuracy and the domain-invariance.

IV. CONCLUSIONS

During the past decade, automatic detection and classification of pathological voices has achieved outstanding performances with the advance of machine learning methods. Nevertheless, two main challenges took place in practical applications: (1) state-of-the-art models oftentimes require increased memory loads and computational costs, whereas the resources are rather limited on embedded systems, and (2) the domain mismatch between training and real-world data largely degrades a model's performance. To address these issues, we utilized separable convolutional layers and DAT to build a compressed and domain-robust system. Six experiments were conducted and compared. The effect of λ was also discussed. We therefore proposed an unsupervised domain adaptation system, jointly trained by sufficient labeled data in the source domain and a small amount of unlabeled data in the target domain. The results showed that our system achieved comparable UAR in the target domain (78.9%) to the source domain (80.0%). In addition, the numbers of parameters and MACs were largely reduced by 73.9% and 77.0%, respectively. It is to conclude that our proposed system efficiently reduced computational and memory usage, and effectively eliminated the domain mismatch.

REFERENCES

[1] J. K. Laguaite, "Adult voice screening," *Journal of Speech and Hearing Disorders*, vol. 37, no. 2, pp. 147–151, 1972.

[2] D. E. Morley, "A ten-year survey of speech disorders among university students," *Journal of Speech and Hearing disorders*, vol. 17, no. 1, pp. 25–31, 1952.

[3] L. O. Ramig and K. Verdolini, "Treatment efficacy: voice disorders," *Journal of Speech, Language, and Hearing Research*, vol. 41, no. 1, pp. S101–S116, 1998.

[4] N. Roy, R. M. Merrill, S. D. Gray, and E. M. Smith, "Voice disorders in the general population: prevalence, risk factors, and occupational impact," *The Laryngoscope*, vol. 115, no. 11, pp. 1988–1995, 2005.

[5] S. M. Cohen, "Self-reported impact of dysphonia in a primary care population: An epidemiological study," *The Laryngoscope*, vol. 120, no. 10, pp. 2022–2032, 2010.

[6] S. R. Best and C. Fakhry, "The prevalence, diagnosis, and management of voice disorders in a national ambulatory medical care survey (names) cohort," *The Laryngoscope*, vol. 121, no. 1, pp. 150–157, 2011.

[7] S. M. Cohen, J. Kim, N. Roy, C. Asche, and M. Courey, "Prevalence and causes of dysphonia in a large treatment-seeking population," *The Laryngoscope*, vol. 122, no. 2, pp. 343–348, 2012.

[8] A. A. Dibazar, S. Narayanan, and T. W. Berger, "Feature analysis for automatic detection of pathological speech," in *Proceedings of the Second Joint 24th Annual Conference and the Annual Fall Meeting of the Biomedical Engineering Society [Engineering in Medicine and Biology]*, vol. 1, pp. 182–183, IEEE, 2002.

[9] P. Henríquez, J. B. Alonso, M. A. Ferrer, C. M. Travieso, J. I. Godino-Llorente, and F. Díaz-de María, "Characterization of healthy and pathological voice through measures based on nonlinear dynamics," *IEEE transactions on audio, speech, and language processing*, vol. 17, no. 6, pp. 1186–1195, 2009.

[10] G. Vaziri, F. Almasganj, and R. Behroozmand, "Pathological assessment of patients' speech signals using nonlinear dynamical analysis," *Computers in biology and medicine*, vol. 40, no. 1, pp. 54–63, 2010.

[11] K. Umamathy, S. Krishnan, V. Parsa, and D. G. Jamieson, "Discrimination of pathological voices using a time-frequency approach," *IEEE Transactions on Biomedical Engineering*, vol. 52, no. 3, pp. 421–430, 2005.

[12] R. Fraile, N. Sáenz-Lechón, J. I. Godino-Llorente, V. Osma-Ruiz, and C. Fredouille, "Automatic detection of laryngeal pathologies in records of sustained vowels by means of Mel-frequency cepstral coefficient parameters and differentiation of patients by sex," *Folia phoniatrica et logopaedica*, vol. 61, no. 3, pp. 146–152, 2009.

[13] J. I. Godino-Llorente, P. Gomez-Vilda, and M. Blanco-Velasco, "Dimensionality reduction of a pathological voice quality assessment system based on gaussian mixture models and short-term cepstral parameters," *IEEE transactions on biomedical engineering*, vol. 53, no. 10, pp. 1943–1953, 2006.

[14] S. C. Costa, B. G. A. Neto, and J. M. Fachine, "Pathological voice discrimination using cepstral analysis, vector quantization and hidden markov models," in *2008 8th IEEE International Conference on Bioinformatics and BioEngineering*, pp. 1–5, IEEE, 2008.

[15] L. Salhi, T. Mourad, and A. Cherif, "Voice disorders identification using multilayer neural network," *pathology*, vol. 2, no. 7, p. 8, 2010.

[16] M. K. Arjmandi and M. Pooyan, "An optimum algorithm in pathological voice quality assessment using wavelet-packet-based features, linear discriminant analysis and support vector machine," *Biomedical Signal Processing and Control*, vol. 7, no. 1, pp. 3–19, 2012.

[17] M. Markaki and Y. Stylianou, "Using modulation spectra for voice pathology detection and classification," in *2009 Annual International Conference of the IEEE Engineering in Medicine and Biology Society*, pp. 2514–2517, IEEE, 2009.

[18] M. Markaki and Y. Stylianou, "Voice pathology detection and discrimination based on modulation spectral features," *IEEE Transactions on audio, speech, and language processing*, vol. 19, no. 7, pp. 1938–1948, 2011.

[19] I. Hammami, L. Salhi, and S. Labidi, "Pathological voices detection using support vector machine," in *2016 2nd International Conference on Advanced Technologies for Signal and Image Processing (ATSIP)*, pp. 662–666, IEEE, 2016.

[20] L. Verde, G. De Pietro, and G. Sannino, "Voice disorder identification by using machine learning techniques," *IEEE access*, vol. 6, pp. 16246–16255, 2018.

[21] M. Pishgar, F. Karim, S. Majumdar, and H. Darabi, "Pathological voice classification using Mel-cepstrum vectors and support vector machine," *arXiv preprint arXiv:1812.07729*, 2018.

[22] J. D. Arias-Londoño, J. I. Godino-Llorente, M. Markaki, and Y. Stylianou, "On combining information from modulation spectra and Mel-frequency cepstral coefficients for automatic detection of patholog-

- ical voices,” *Logopedics Phoniatrics Vocology*, vol. 36, no. 2, pp. 60–69, 2011.
- [23] J. D. Arias-Londoño, J. I. Godino-Llorente, N. Sáenz-Lechón, V. Osma-Ruiz, and G. Castellanos-Domínguez, “Automatic detection of pathological voices using complexity measures, noise parameters, and Mel-cepstral coefficients,” *IEEE Transactions on biomedical engineering*, vol. 58, no. 2, pp. 370–379, 2010.
- [24] M. Dahmani and M. Guerti, “Vocal folds pathologies classification using naïve bayes networks,” in *2017 6th international conference on systems and control (ICSC)*, pp. 426–432, IEEE, 2017.
- [25] M. Dahmani and M. Guerti, “Glottal signal parameters as features set for neurological voice disorders diagnosis using K-nearest neighbors (KNN),” in *2018 2nd International Conference on Natural Language and Speech Processing (ICNLSP)*, pp. 1–5, IEEE, 2018.
- [26] H. Wu, J. Soraghan, A. Lowit, and G. Di Caterina, “A deep learning method for pathological voice detection using convolutional deep belief networks,” *Interspeech 2018*, 2018.
- [27] H. Wu, J. Soraghan, A. Lowit, and G. Di Caterina, “Convolutional neural networks for pathological voice detection,” in *2018 40th annual international conference of the IEEE engineering in medicine and biology society (EMBC)*, pp. 1–4, IEEE, 2018.
- [28] V. Gupta, “Voice disorder detection using long short term memory (LSTM) model,” *arXiv preprint arXiv:1812.01779*, 2018.
- [29] S.-H. Fang, Y. Tsao, M.-J. Hsiao, J.-Y. Chen, Y.-H. Lai, F.-C. Lin, and C.-T. Wang, “Detection of pathological voice using cepstrum vectors: A deep learning approach,” *Journal of Voice*, vol. 33, no. 5, pp. 634–641, 2019.
- [30] T. Lee, Y. Liu, P.-W. Huang, J.-T. Chien, W. K. Lam, Y. T. Yeung, T. K. Law, K. Y. Lee, A. P.-H. Kong, and S.-P. Law, “Automatic speech recognition for acoustical analysis and assessment of cantonese pathological voice and speech,” in *2016 IEEE international conference on acoustics, speech and signal processing (ICASSP)*, pp. 6475–6479, IEEE, 2016.
- [31] Y.-T. Hsu, Z. Zhu, C.-T. Wang, S.-H. Fang, F. Rudzicz, and Y. Tsao, “Robustness against the channel effect in pathological voice detection,” *arXiv preprint arXiv:1811.10376*, 2018.
- [32] M. Pham, J. Lin, and Y. Zhang, “Diagnosing voice disorder with machine learning,” in *2018 IEEE International Conference on Big Data (Big Data)*, pp. 5263–5266, IEEE, 2018.
- [33] T. Grzywalski, A. Maciaszek, A. Biniakowski, J. Orwat, S. Drgas, M. Piecuch, R. Belluzzo, K. Joachimiak, D. Niemiec, J. Ptaszynski, *et al.*, “Parameterization of sequence of mfccs for dnn-based voice disorder detection,” in *2018 IEEE International conference on big data (big data)*, pp. 5247–5251, IEEE, 2018.
- [34] C. Bhat and S. K. Koppurapu, “FEMH voice data challenge: Voice disorder detection and classification using acoustic descriptors,” in *2018 IEEE International Conference on Big Data (Big Data)*, pp. 5233–5237, IEEE, 2018.
- [35] K. Degila, R. Errattahi, and A. El Hannani, “The UCD system for the 2018 FEMH voice data challenge,” in *2018 IEEE International Conference on Big Data (Big Data)*, pp. 5242–5246, IEEE, 2018.
- [36] J. D. Arias-Londoño, J. A. Gómez-García, L. Moro-Velázquez, and J. I. Godino-Llorente, “Byovoz automatic voice condition analysis system for the 2018 FEMH challenge,” in *2018 IEEE International Conference on Big Data (Big Data)*, pp. 5228–5232, IEEE, 2018.
- [37] K. A. Islam, D. Perez, and J. Li, “A transfer learning approach for the 2018 FEMH voice data challenge,” in *2018 IEEE International Conference on Big Data (Big Data)*, pp. 5252–5257, IEEE, 2018.
- [38] A. Ramalingam, S. Kedari, and C. Vuppapapati, “Ieee femh voice data challenge 2018,” in *2018 IEEE International Conference on Big Data (Big Data)*, pp. 5272–5276, IEEE, 2018.
- [39] B. Jacob, S. Kligys, B. Chen, M. Zhu, M. Tang, A. Howard, H. Adam, and D. Kalenichenko, “Quantization and training of neural networks for efficient integer-arithmetic-only inference,” in *Proceedings of the IEEE conference on computer vision and pattern recognition*, pp. 2704–2713, 2018.
- [40] Y.-T. Hsu, Y.-C. Lin, S.-W. Fu, Y. Tsao, and T.-W. Kuo, “A study on speech enhancement using exponent-only floating point quantized neural network (EOFP-QNN),” in *2018 IEEE Spoken Language Technology Workshop (SLT)*, pp. 566–573, IEEE, 2018.
- [41] G. Hinton, O. Vinyals, and J. Dean, “Distilling the knowledge in a neural network,” *arXiv preprint arXiv:1503.02531*, 2015.
- [42] M. Wang, B. Liu, and H. Foroosh, “Factorized convolutional neural networks,” in *Proceedings of the IEEE International Conference on Computer Vision Workshops*, pp. 545–553, 2017.
- [43] E. Romera, J. M. Alvarez, L. M. Bergasa, and R. Arroyo, “Erfnet: Efficient residual factorized convnet for real-time semantic segmentation,” *IEEE Transactions on Intelligent Transportation Systems*, vol. 19, no. 1, pp. 263–272, 2017.
- [44] A. G. Howard, M. Zhu, B. Chen, D. Kalenichenko, W. Wang, T. Weyand, M. Andreetto, and H. Adam, “Mobilenets: Efficient convolutional neural networks for mobile vision applications,” *arXiv preprint arXiv:1704.04861*, 2017.
- [45] E. Tzeng, J. Hoffman, N. Zhang, K. Saenko, and T. Darrell, “Deep domain confusion: Maximizing for domain invariance,” *arXiv preprint arXiv:1412.3474*, 2014.
- [46] Y. Ganin, E. Ustinova, H. Ajakan, P. Germain, H. Larochelle, F. Laviolette, M. Marchand, and V. Lempitsky, “Domain-adversarial training of neural networks,” *The journal of machine learning research*, vol. 17, no. 1, pp. 2096–2030, 2016.
- [47] S. Ruder, “An overview of gradient descent optimization algorithms,” *arXiv preprint arXiv:1609.04747*, 2016.
- [48] S. Ioffe and C. Szegedy, “Batch normalization: Accelerating deep network training by reducing internal covariate shift,” in *International conference on machine learning*, pp. 448–456, PMLR, 2015.
- [49] B. Xu, N. Wang, T. Chen, and M. Li, “Empirical evaluation of rectified activations in convolutional network,” *arXiv preprint arXiv:1505.00853*, 2015.
- [50] D. P. Kingma and J. Ba, “Adam: A method for stochastic optimization,” *arXiv preprint arXiv:1412.6980*, 2014.
- [51] T.-T. Wong, “Performance evaluation of classification algorithms by k-fold and leave-one-out cross validation,” *Pattern Recognition*, vol. 48, no. 9, pp. 2839–2846, 2015.